# Bispectral Interreflection Estimation of Fluorescent Objects

***Shoji Tominaga, Keiji Kato, Keita Hirai, and Takahiko Horiuchi;***
***Graduate School of Advanced Integration Science, Chiba University, Chiba, Japan***

## Abstract

*If multiple objects are located closely, we often observe interreflection on the object surfaces. The interreflection is accompanied by a change in the appearance of the object surfaces. In this paper, we propose a method to estimate the spectral image components from the captured images of two closely apposed objects. A spectral imaging system is used for image capturing of both objects under uniform illumination. First, we describe the basis bispectral characteristics of a fluorescent object. Second, we model the interreflection of two objects with the bispectral characteristics. The surface appearance of each object was based on both reflected component and luminescent component. We show that the spectral composition of interreflection is determined by a series of multiplication of the Donaldson matrices of the two objects. The spectral components of one bounce interreflection can be limited to only four spectral functions. Third, an algorithm is developed to estimate the spectral image components from the observed spectral radiance images that are influenced by the interreflection. The algorithm is based on a two-step estimation procedure in which the spectral components are estimated separately in the outside and inside of the emission wavelength range. The feasibility of the proposed method is investigated using fluorescent samples in details.*

## Introduction

Objects containing fluorescence are widely available in our daily life. Fluorescent materials are used in painted objects, papers, plastics, stationeries, clothes, shoes and all sorts of things that we may come across each day. The material appearance of a fluorescent object is more attractive and provides much better impression compared to a non-fluorescent object. Fluorescence is a luminous phenomenon where a material is first excited by the electromagnetic radiation in a specific wavelength region, and then the excited state relaxation emits the electromagnetic radiation in another longer wavelength region [1]. This shift of wavelength, called Stokes shift [2], causes a compelling visual effect, when it occurs within the visible range. In particular, many fluorescent objects appear brighter and more vivid than the original object color based on a non-fluorescent light reflection.

The fluorescent characteristics are described in terms of the bispectral radiance factor. The radiance factor is a function of two wavelength variables: the excitation wavelength of incident light and the emission/reflection wavelength. The two-dimensional characteristics are summarized as a Donaldson matrix [3],[4], which is an illuminant invariant matrix representation of the bispectral radiance factor of a target object. Traditionally, the Donaldson matrix was measured using two monochromators [5]. However the two-monochromator method is time-consuming and expensive, although it is precise. Tominaga et al. proposed an effective method to estimate the Donaldson matrix based on only two sets of spectral sensor outputs under two different illuminants [6]-[8].

A scene is never composed by one single object alone but always contributed by many different objects. When multiple objects are located closely, there is often interreflection observed on the object surfaces. The interreflection is accompanied by a change in the appearance of the object surfaces. The problems of interreflection detection, analysis, and estimation have been studied in color imaging [9] and computer vision [10]. However, in the previous studies, non-fluorescent objects were being used such as inhomogeneous dielectric and perfect diffuser with Lambertian surface. In such a case, when two matte surfaces are located closely, the color signals observed from one surface consists of two components of the diffuse reflection by direct illumination and the diffuse-to-diffuse interreflection by indirect illumination. The diffuse-to-diffuse interreflection component was often neglected because it is weak compared with the former body reflection. However, if the object colors of the two surfaces are similar to each other, the interreflection effect cannot be neglected. As a fluorescent object has a bispectral characteristic, the previous methods is not suitable for interreflection analysis of fluorescent objects. We note that a fluorescent material emits bright light, and the interreflection with the other surface can essentially change the original material appearance. Therefore the interreflection effects should not be neglected.

The present paper proposes a method to estimate the spectral image components from the captured images of two closely apposed object surfaces. We suppose that the two objects are fluorescent objects with uniform surfaces of different bispectral characteristics. A spectral imaging system is used for image capturing of both objects under uniform illumination. First, we describe briefly the basis bispectral characteristics of a fluorescent object. Second, we model the bispectral interreflection. The spectral composition of interreflection is determined by a series of multiplication of the Donaldson matrices of two objects. We show that the observed spectral images with interreflection can be modeled by combining several bispectral basis functions. Third, an algorithm is developed to estimate the spectral image components from the observed spectral radiance images that are influenced by the interreflection. The algorithm is based on a two-step estimation procedure in which the spectral components are estimated separately in the outside and inside of the emission wavelength range.

## Basic Bispectral Characteristics

The Donaldson matrix represents the bispectral radiance factor of a fluorescent object as a two-variable function of the excitation wavelength $\lambda_{in}$ and the emission/reflection wavelength $\lambda_{out}$ . Figure 1 illustrates the Donaldson matrix $D(\lambda_{out}, \lambda_{in})$ of a yellow paint containing a fluorescent color. This matrix was based on measurements using a bispectrometer system in the range [350,

700nm] with 5nm intervals, where monochromatic light corresponding to each excitation wavelength was projected on the surface. A hump in the emission wavelength [500, 600nm] represents the luminescent radiance factor $D_L(\lambda_{out},\lambda_{in})$ . The spectral radiance factor is also a function of both emission and excitation wavelengths $(\lambda_{out},\lambda_{in})$ . It is known that the normalized spectral curves of the emission component have an input wavelength-independent distribution. Therefore, the luminescent radiance factor can be separated into the emission and excitation wavelength components as $D_L(\lambda_{out},\lambda_{in})=\alpha(\lambda_{out})\beta(\lambda_{in})$ . Figure 2 depicts the relative spectral curves of $\beta(\lambda)$ and $\alpha(\lambda)$ for the yellow fluorescent paint sample on a single wavelength scale. The excitation spectrum $\beta(\lambda)$ is located at shorter wavelength than the emission spectrum $\alpha(\lambda)$ .

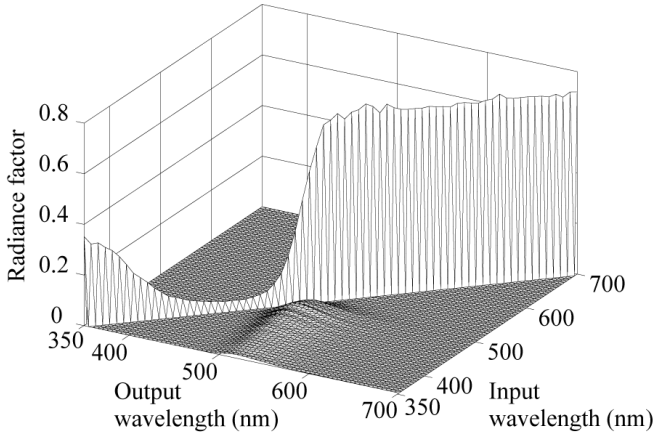


***Figure 1**. Bispectral Donaldson matrix obtained from a yellow paint containing a fluorescent color.*

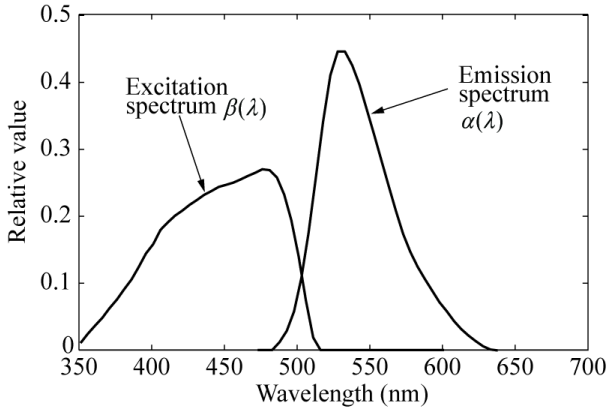


***Figure 2**. Relative spectral curves of the excitation and emission components of a fluorescent paint sample on a single wavelength scale.*

A general form of the Donaldson matrix can be represented in an $N \times N$ matrix as

$$\mathbf{D}=\mathbf{D}_{\mathrm{R}}+\mathbf{D}_{\mathrm{L}} = \begin{bmatrix} s_1 & 0 & \cdots & 0 \\ 0 & s_2 & \ddots & \vdots \\ \vdots & \ddots & \ddots & 0 \\ 0 & \cdots & 0 & s_N \end{bmatrix} + \begin{bmatrix} 0 & & \cdots & & 0 \\ \alpha_2\beta_1 & 0 & & & \\ \alpha_3\beta_1 & \alpha_3\beta_2 & 0 & & \vdots \\ \vdots & \vdots & \ddots & \ddots & \\ \alpha_N\beta_1 & \alpha_N\beta_2 & \cdots & \alpha_N\beta_{N-1} & 0 \end{bmatrix}, \quad (1)$$

where $\mathbf{D}_{\mathrm{R}}$ is a diagonal matrix with elements $s_i$ ($i$=2, 3, .., $N$) representing the reflected radiance factor, and $\mathbf{D}_{\mathrm{L}}$ is a triangular matrix with elements $\alpha_i$ ($i$ = 2, 3, .., $N$), and $\beta_i$ ($i$ = 1, 2, .., $N$ - 1) representing the emission spectrum and the excitation spectrum. Tominaga et al. [7],[8] proposed a method to estimate the Donaldson matrix **D** by using two illuminant projections.

## Bispectral Interreflection Model

The surface appearance of a fluorescent object consists of both reflected and luminescent components. When we assume a Lambert surface, the reflected component of the observation at a surface point $x$ is described as

$$y_R(x,\lambda)=S(\lambda)\cos\theta E(\lambda) \quad (2)$$

where $E(\lambda)$ is the spectral power distribution of illuminant, and $\theta$ is the angel of incidence. On the other hand, concerning the directional characteristics of the luminescent radiance factor, it was found that the characteristic is similar to the reflection characteristic for a Lambertian surface [11]. That is, the luminescent radiance is proportional only to the cosine of incident angle, independently of the viewing angle as

$$y_L(x,\lambda_{out},\lambda_{in})=D_L(\lambda_{out},\lambda_{in})\cos\theta E(\lambda) . \quad (3)$$

Therefore, the observation of bispectral bidirectional radiance factor of a fluorescent object surface can be summarized as a continuous function of wavelength

$$y(x,\lambda_{out})= S(\lambda)\delta(\lambda_{out}-\lambda_{in})\cos\theta E(\lambda_{in})+\alpha(\lambda_{out})\cos\theta\int\beta(\lambda_{in})E(\lambda_{in})d\lambda_{in} . \quad (4)$$

Let us suppose two fluorescent objects located closely as shown in Figure 3, where interreflection occurs between two surfaces with different bispectral characteristics. The two surfaces are uniform matte surfaces, which are illuminated uniformly with a single light source. The spectral composition of the interreflection between two fluorescent objects is determined by a series of multiplication of the Donaldson matrices $\mathbf{D}_1$ and $\mathbf{D}_2$ such as $\cdots\mathbf{D}_1\mathbf{D}_2\mathbf{D}_1$ or $\cdots\mathbf{D}_2\mathbf{D}_1\mathbf{D}_2$ . First, the spectral composition observed from the two surfaces 1 and 2 by direct illumination as described as

$$\begin{aligned}\mathbf{y}_1&=\mathbf{D}_1\mathbf{e}\\ \mathbf{y}_2&=\mathbf{D}_2\mathbf{e}\end{aligned}, \quad (5)$$

where **e** denotes an $N$-dimensional illuminant vector. Next, each nearby surface provides a second source of illumination onto the other surface. Suppose that the interreflection is based on one bounce between the two surfaces. In this case we have

$$\begin{aligned}\mathbf{y}_1 &= \mathbf{D}_1\mathbf{e} + \mathbf{D}_1\mathbf{D}_2\mathbf{e} \\ &= \{(\mathbf{D}_{R1} + \mathbf{D}_{L1}) + (\mathbf{D}_{R1} + \mathbf{D}_{L1})(\mathbf{D}_{R2} + \mathbf{D}_{L2})\}\mathbf{e} \\ \mathbf{y}_2 &= \mathbf{D}_2\mathbf{e} + \mathbf{D}_2\mathbf{D}_1\mathbf{e} \\ &= \{(\mathbf{D}_{R2} + \mathbf{D}_{L2}) + (\mathbf{D}_{R2} + \mathbf{D}_{L2})(\mathbf{D}_{R1} + \mathbf{D}_{L1})\}\mathbf{e}\end{aligned} \tag{6}$$

where $\mathbf{D}_1\mathbf{e}$ ( $\mathbf{D}_2\mathbf{e}$ ) in the right-hand side represents the bispectral radiance factor by direct illumination, and $\mathbf{D}_1\mathbf{D}_2\mathbf{e}$ ( $\mathbf{D}_2\mathbf{D}_1\mathbf{e}$ ) represents the interreflection component by the light illuminated by the other surface, which has also the bispectral characteristics of the reflected and luminescent radiance factors.

The detailed inspection of the spectral composition in Eq.(6) leads to the following properties:

(1) $[\mathbf{D}_{R1}\mathbf{D}_{R2}\mathbf{e}]$ represents the diffuse-diffuse interreflection based on diffuse reflection of both surfaces.

(2) $[\mathbf{D}_{R1}\mathbf{D}_{L2}\mathbf{e}]$ represents the reflection on Surface 1 which is illuminated by fluorescence from Surface 2.

(3) $[\mathbf{D}_{L1}\mathbf{D}_{R2}\mathbf{e}]$ represents the luminescent emission from Surface 1 which is excited by reflection of Surfaces 2. Therefore the spectral composition is coincident with $\alpha_1(\lambda)$.

(4) $[\mathbf{D}_{L2}\mathbf{D}_{R1}\mathbf{e}]$ has the same property on Surface 2 as $[\mathbf{D}_{L1}\mathbf{D}_{R2}\mathbf{e}]$ in (3).

(5) $[\mathbf{D}_{R2}\mathbf{D}_{L1}\mathbf{e}]$ has the same property on Surface 2 as $[\mathbf{D}_{R1}\mathbf{D}_{L2}\mathbf{e}]$ in (2).

(6) $[\mathbf{D}_{L1}\mathbf{D}_{L2}\mathbf{e}]$ represents the fluorescent emission on Surface 1 caused by fluorescent excitation on Surface 2. Therefore, it has the same spectral composition as $\alpha_1(\lambda)$. Note that this term disappear if the emission wavelength of Surface 1 is longer than the excitation wavelength of Surface2, that is $\beta_1(\lambda) < \alpha_2(\lambda)$.

(7) $[\mathbf{D}_{L2}\mathbf{D}_{L1}\mathbf{e}]$ has the same property on Surface 2 as $[\mathbf{D}_{L1}\mathbf{D}_{L2}\mathbf{e}]$ in (6). The spectral composition is $\alpha_2(\lambda)$. This term is effective only if the emission wavelength of Surface 2 is in the range of the excitation wavelength of Surface 1.

On the basis of the above findings, we describe the spectral model of interreflection by the continuous functions of wavelength rather than the matrix notation. The observations of spectral radiances at location $x$ of Surface 1 and Surface 2 are represented as

$$\begin{aligned}y_1(x,\lambda) &= f_{11}(x)S_1(\lambda)E(\lambda) + f_{11e}(x)\alpha_1(\lambda) + f_{12}(x)S_1(\lambda)S_2(\lambda)E(\lambda) \\ &\quad + f_{13e}(x)S_1(\lambda)\alpha_2(\lambda) + f_{14e}(x)\alpha_1(\lambda) + f_{15e}(x)\alpha_1(\lambda) \\ y_2(x,\lambda) &= f_{21}(x)S_2(\lambda)E(\lambda) + f_{21e}(x)\alpha_2(\lambda) + f_{22}(x)S_1(\lambda)S_2(\lambda)E(\lambda) \\ &\quad + f_{23e}(x)S_2(\lambda)\alpha_1(\lambda) + f_{24e}(x)\alpha_2(\lambda) + f_{25e}(x)\alpha_2(\lambda)\end{aligned}, \tag{7}$$

where all weights $f(x)$ with variable of location $x$ represent geometric form factors, which depend on the surface shapes and distance between the two surfaces. In the right-hand side in Eq.(7), four terms from $f_{12}(x)S_1(\lambda)S_2(\lambda)E(\lambda)$ to $f_{15e}(x)\alpha_1(\lambda)$ correspond to from (1) to (4) in the above terms, respectively. The weights $f_{11}(x)$, $f_{12}(x)$, $f_{21}(x)$, and $f_{22}(x)$ are independent of illuminant. On the other hand, note that the weights $f_{11e}(x)$, $f_{13e}(x)$, $f_{14e}(x)$, $f_{15e}(x)$, $f_{21e}(x)$, $f_{23e}(x)$, $f_{24e}(x)$, and $f_{25e}(x)$ are dependent of illuminant. Grouping the spectral components yields a spectral radiance containing only four terms

$$\begin{aligned}y_1(x,\lambda) &= f_{11}(x)S_1(\lambda)E(\lambda) + f_{12}(x)S_1(\lambda)S_2(\lambda)E(\lambda) \\ &\quad + f_{13e}(x)S_1(\lambda)\alpha_2(\lambda) + f_{14e}(x)\alpha_1(\lambda) \\ y_2(x,\lambda) &= f_{21}(x)S_2(\lambda)E(\lambda) + f_{22}(x)S_1(\lambda)S_2(\lambda)E(\lambda) \\ &\quad + f_{23e}(x)S_2(\lambda)\alpha_1(\lambda) + f_{24e}(x)\alpha_2(\lambda)\end{aligned}. \tag{8}$$

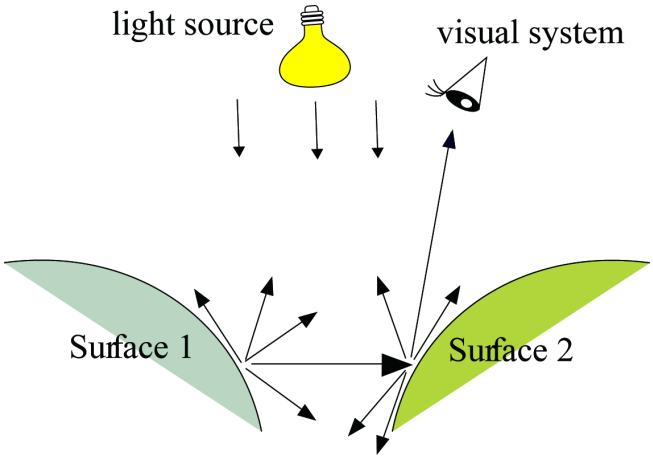


***Figure 3**. Interreflection between two surfaces with different bispectral characteristics.*

## Spectral Composition Estimation

If we know the bispectral characteristics of both materials (or we can estimate these by a different way), the weights at every location are then estimated from the observations. As a result, the observed spectral radiance image can be decomposed into several spectral component images, depending on the type of interreflection effects.

For making numerical computation easy, we rewrite the above equations into a matrix equation using *N*-dimensional vectors as

$$\begin{aligned}\mathbf{y}_1 &= \mathbf{A}_1\mathbf{f}_1 \\ \mathbf{y}_2 &= \mathbf{A}_2\mathbf{f}_2\end{aligned} \tag{9}$$

where

$$\begin{aligned}\mathbf{A}_1 &= [\mathbf{s}_1.\mathbf{e},\ \mathbf{s}_1.\mathbf{s}_2.\mathbf{e},\ \boldsymbol{\alpha}_1, \mathbf{s}_1.\boldsymbol{\alpha}_2\ ],\ \mathbf{f}_1 = [f_{11}, f_{12}, f_{13e}, f_{14e}]^t \\ \mathbf{A}_2 &= [\mathbf{s}_2.\mathbf{e},\ \mathbf{s}_1.\mathbf{s}_2.\mathbf{e},\ \boldsymbol{\alpha}_2, \mathbf{s}_2.\boldsymbol{\alpha}_1],\ \mathbf{f}_2 = [f_{21}, f_{22}, f_{23e}, f_{24e}]^t\end{aligned}. \tag{10}$$

The symbols . and *t* denote element-wise multiplication and matrix transposition, respectively. We note that $f_{14e}$ (also $f_{24e}$) cannot be decomposed further into $(f_{11e}, f_{14e}, f_{15e})$ (also $(f_{21e}, f_{24e}, f_{25e})$). The unknown parameters to be estimated are the four elements in $\mathbf{f}_1$ and $\mathbf{f}_2$. The standard least-squared solutions of Eq.(9) are given in the form

$$\begin{aligned}\hat{\mathbf{f}}_1 &= \left[\mathbf{A}_1{}^t\mathbf{A}_1\right]^{-1}\mathbf{A}_1{}^t\mathbf{y}_1 \\ \hat{\mathbf{f}}_2 &= \left[\mathbf{A}_2{}^t\mathbf{A}_2\right]^{-1}\mathbf{A}_2{}^t\mathbf{y}_2\end{aligned}. \tag{11}$$

By taking the fluorescent characteristics into account, we can device an effective estimation method. First, since $(f_{11}, f_{12})$ and $(f_{21}, f_{22})$ are illuminant-independent parameters, the estimation accuracy is steadily improved by observing the same surfaces under multiple exposures of different light sources.

Second, although the surface spectral reflectance is effective in the entire range of visible wavelength, the emission spectrum is effective only in a limited wavelength range. For example, the emission range in Figure 2 is [480, 630 nm]. Therefore, the model equations in Eq. (9) have only two unknown parameters outside the emission range.

Based on these considerations, we propose a two-step estimation procedure. Suppose the same surfaces are observed under two illuminants A and B. At the first step, the parameters $(f_{11}, f_{12})$ and $(f_{21}, f_{22})$ are estimated by solving the following equations

$$\begin{bmatrix} \mathbf{y}^1_{1A} \\ \mathbf{y}^1_{1B} \end{bmatrix} = \begin{bmatrix} \mathbf{s}^1_1.\mathbf{e}^1_A & \mathbf{s}^1_1.\mathbf{s}^1_2.\mathbf{e}^1_A \\ \mathbf{s}^1_1.\mathbf{e}^1_B & \mathbf{s}^1_1.\mathbf{s}^1_2.\mathbf{e}^1_B \end{bmatrix} \begin{bmatrix} f_{11} \\ f_{12} \end{bmatrix}$$
$$\begin{bmatrix} \mathbf{y}^1_{2A} \\ \mathbf{y}^1_{2B} \end{bmatrix} = \begin{bmatrix} \mathbf{s}^1_2.\mathbf{e}^1_A & \mathbf{s}^1_1.\mathbf{s}^1_2.\mathbf{e}^1_A \\ \mathbf{s}^1_2.\mathbf{e}^1_B & \mathbf{s}^1_1.\mathbf{s}^1_2.\mathbf{e}^1_B \end{bmatrix} \begin{bmatrix} f_{21} \\ f_{22} \end{bmatrix}, \quad (12)$$

where $(\mathbf{y}^1_{1A}, \mathbf{y}^1_{1B})$ and $(\mathbf{y}^1_{2A}, \mathbf{y}^1_{2B})$ denote the observations of Surfaces 1 and 2 under Illuminants A and B, $(\mathbf{e}_A, \mathbf{e}_B)$ denote the spectra of Illuminants A and B, and the super fix 1 denotes spectrum outside the emission range. For the second step, the above estimates $(\hat{f}_{11}, \hat{f}_{12})$ and $(\hat{f}_{21}, \hat{f}_{22})$ are used in estimation of the remaining parameters in the emission range. We have

$$\begin{bmatrix} \mathbf{y}^2_{1A} \\ \mathbf{y}^2_{1B} \end{bmatrix} = \begin{bmatrix} \hat{\mathbf{y}}^2_{1A} \\ \hat{\mathbf{y}}^2_{1B} \end{bmatrix} + \begin{bmatrix} \boldsymbol{\alpha}_1 & \mathbf{0} & \mathbf{s}^2_1.\boldsymbol{\alpha}_2 & \mathbf{0} \\ \mathbf{0} & \boldsymbol{\alpha}_1 & \mathbf{0} & \mathbf{s}^2_1.\boldsymbol{\alpha}_2 \end{bmatrix} \begin{bmatrix} f_{13eA} \\ f_{13eB} \\ f_{14eA} \\ f_{14eB} \end{bmatrix}$$
$$\begin{bmatrix} \mathbf{y}^2_{2A} \\ \mathbf{y}^2_{2B} \end{bmatrix} = \begin{bmatrix} \hat{\mathbf{y}}^2_{2A} \\ \hat{\mathbf{y}}^2_{2B} \end{bmatrix} + \begin{bmatrix} \boldsymbol{\alpha}_2 & \mathbf{0} & \mathbf{s}^2_2.\boldsymbol{\alpha}_1 & \mathbf{0} \\ \mathbf{0} & \boldsymbol{\alpha}_2 & \mathbf{0} & \mathbf{s}^2_2.\boldsymbol{\alpha}_1 \end{bmatrix} \begin{bmatrix} f_{23eA} \\ f_{23eB} \\ f_{24eA} \\ f_{24eB} \end{bmatrix}, \quad (13)$$

where $(\hat{\mathbf{y}}^2_{1A}, \hat{\mathbf{y}}^2_{1B})$ and $(\hat{\mathbf{y}}^2_{2A}, \hat{\mathbf{y}}^2_{2B})$ are the predicted observations in the emission range based on the estimates $(\hat{f}_{11}, \hat{f}_{12})$ and $(\hat{f}_{21}, \hat{f}_{22})$. Note that the emission range can be different between $\boldsymbol{\alpha}_1$ and $\boldsymbol{\alpha}_2$.

The above two-step computation procedure is performed at every location point on both surfaces.

## Experimental Results

One fluorescent sample and one non-fluorescent sample were used in the experiments. The fluorescent sample was made by drawing a fluorescent paint called Lumi-Yellow on a black Kent paper. The Donaldson matrix is shown in Figure 1. The object color is yellow, and the luminescent color is green. The non-fluorescent sample was a standard white reference paper. The two objects were placed at an angle of 90 degrees. The two light sources used in the experiments were an incandescent lamp and an artificial sun light lamp. The objects were illuminated from the front by the respective light sources. We used a spectral imaging system, consisting of a monochrome camera, a LCT filter, and a personal computer. This imaging system was operated in the visible range [400, 700 nm]. The spectral images were captured at equal intervals of 5nm.

Figure 4 shows the observed color image of a fluorescent object (left) and a non-fluorescent object (right) under the artificial sunlight illumination. We can see that interreflection effects appear in the region close to the intersection between the two surfaces. First, the Donaldson matrices for two objects were determined at two locations having little interreflection effects which were distant from the intersection. Our previous method [8] was applied to the spectral image data in order to obtain the spectral reflectance $S_1(\lambda)$ and the emission spectrum $\alpha_1(\lambda)$ of the fluorescent object and the reflectance $S_2(\lambda)$ of the non-fluorescent object. Then, the proposed two-step estimation algorithm was applied to all pixels of the observed spectral images by using the obtained spectral curves $S_1(\lambda)$, $\alpha_1(\lambda)$, and $S_2(\lambda)$. The emission range was determined as [380, 650 nm].

***Figure 4.*** *I Observed color image of a fluorescent object (left) and a non-fluorescent object (right) under the artificial sunlight illumination. Interreflection effects appear in the region close to the intersection.*

Figure 5 shows the estimated weighting coefficients as color images, where (a) represents $(\hat{f}_{11}, \hat{f}_{21})$ for the diffuse reflection, (b) represents $(\hat{f}_{12}, \hat{f}_{22})$ for the diffuse-diffuse interreflection, (c) represents $(f_{13eA}, f_{23eA})$ for fluorescent emission (left) and interreflection (right) under the incandescent light, and (d) represents $(\hat{f}_{13eB}, \hat{f}_{23eB})$ for fluorescent emission (left) and interreflection (right) under the artificial sunlight. Finally, Figure 6 demonstrates the component images of the observations for the two objects under the artificial sunlight, in which (a) represents the body color component based on the diffuse reflection without interreflection effect, (b) represents the diffuse-diffuse interreflection component, and (c) represents the fluorescent component. We should note that the left half in Figure 6(c) consists of the fluorescent emission which is caused by direct illumination and indirect illumination from the right surface. Also, note in the right half in Figure 6(c) that the fluorescent color is projected onto the white surface. Figure 6(d) shows the combined image by summing the three component images. Note that this image approximates well the observed image in Figure 4.

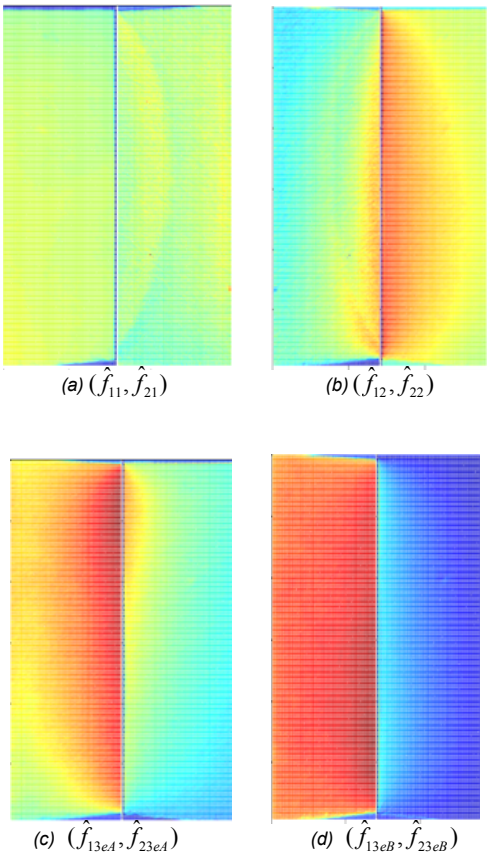


***Figure 5**. Estimated weighting coefficients*

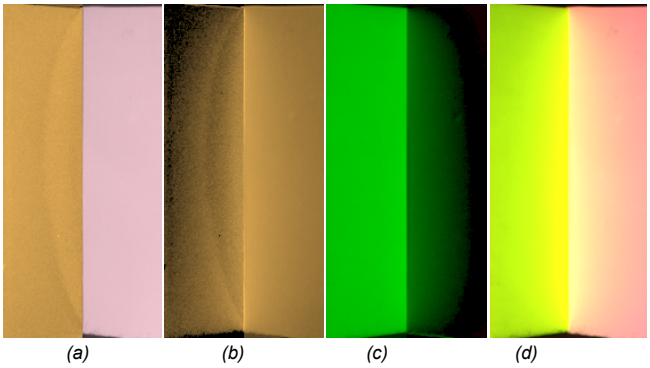


***Figure 6**. Component images of the observed color image under the artificial sunlight. (a) diffuse reflection without interreflection, (b) diffuse-diffuse interreflection, (c) fluorescent emission, (d) combined image by summing three components.*

## Conclusion

In this paper we have proposed a method to estimate the spectral image components from the captured images of two closely apposed object surfaces. We supposed that the objects with uniform surfaces contained different bispectral characteristics of fluorescence. A spectral imaging system was used for image capturing of both objects under uniform illumination. First, we described briefly the basis bispectral characteristics of a fluorescent object. Second, we model the interreflection of two objects with the bispectral characteristics. The surface appearance of each object was based on both reflected component and luminescent component. The spectral composition of interreflection was determined by a series of multiplication of the Donaldson matrices of two objects. We found that grouping the spectral components yields a spectral radiance containing only four terms. Third, an algorithm was developed to estimate the spectral image components from the observed spectral radiance images that were influenced by interreflection. The algorithm was based on a two-step estimation procedure in which the spectral components were estimated separately in the outside and inside of the emission wavelength range. The feasibility of the proposed method was demonstrated using fluorescent samples in details.

## Acknowledgments

This work was supported by JSPS KAKENHI Grant Number 25540063.

## References

[1] G. Wyszecki and W. S. Stiles, Color Science: Concepts and Methods, Quantitative Data and Formulae (Wiley, New York, 1982).
[2] J. R. Lakowicz, Principles of Fluorescence Spectroscopy, Third ed., (Springer, 2006).
[3] R. Donaldson, Spectrophotometry of fluorescent pigments, British J. of Applied Physics, 5, pg.210, (1954).
[4] F. W. Billmeyer, Jr. and T. F. Chong, Calculation of the spectral radiance factors of uminescent samples, Color Res. Appl. 5, pg.156 (1980).
[5] J. Mutanen, Fluorescent Colors, Ph.D. Dissertation, Department of Physics, 45, Univ. of Joensuu, (2004).
[6] S. Tominaga, T. Horiuchi and T. Kamiyama, Spectral estimation of fluorescent objects using visible lights and an imaging device, Proc. CIC19, pg. 352. (2011).
[7] S. Tominaga, K. Hirai, and T. Horiuchi, Estimation of Bispectral Matrix for Fluorescent Objects. Proc. CVCS2013, pg.1. (2013).
[8] S. Tominaga, K. Hirai, and T. Horiuchi, Estimation of bispectral Donaldson matrices of fluorescent objects by using two illuminant projections, J. Optical Society of America A, 32, pg. 1068-1078 (2015)
[9] S. Tominaga, Separation of Reflection Components from a Color Image, Proc. CIC5, pg. 354. (1997).
[10] R. Bajcsy, S.W. Lee, and A. Leonards, Detection of diffuse and specular interface reflections and inter-reflections by color image segmentation, Int. J. Computer Vision, 17, pg.241, (1996).
[11] S. Tominaga, K. Hirai and T. Horiuchi, Measurement and Modeling of Bidirectional Characteristics of Fluorescent Objects, Lecture Notes in Computer Science, LNCS8509 (Springer-Verlag, 2014), pg. 35.

## Author Biography

*Shoji Tominaga received the B.E., M.S., and Ph.D. degrees in electrical engineering from Osaka University, Osaka, Japan, in 1970, 1972, and 1975, respectively. In 2006, he joined Chiba University, Japan, where he was a Professor (2006-2013) and Dean (2011-2013) at Graduate School of Advanced Integration Science. He is now a Specially Appointed Researcher, Chiba University. His research interests include digital color imaging, multispectral image analysis, and material appearance modeling. He is a Fellow of IEEE, IS&T, and SPIE.*